



4-Phenoxypiperidine pyridazin-3-one histamine H₃ receptor inverse agonists demonstrating potent and robust wake promoting activity

Robert L. Hudkins*, Allison L. Zulli, Reddeppa reddy Dandu, Ming Tao, Kurt A. Josef, Lisa D. Aimone, R. Curtis Haltiwanger, Zeqi Huang, Jacquelyn A. Lyons, Joanne R. Mathiasen, Rita Raddatz, John A. Gruner

Discovery Research, Cephalon, Inc., 145 Brandywine Parkway, West Chester, PA 19380, USA

ARTICLE INFO

Article history:

Received 22 November 2011

Revised 4 January 2012

Accepted 9 January 2012

Available online 13 January 2012

Keywords:

Histamine H₃ receptor

H₃ inverse agonist

Pyridazin-3-one

CEP-26401

Irdabisant

Sleep–wake

ABSTRACT

Structure–activity relationships for a series of phenoxypiperidine pyridazin-3-one H₃R antagonists/inverse agonists are disclosed. The search for compounds with improved hERG and DAT selectivity without the formation of in vivo active metabolites identified 6-[4-(1-cyclobutyl-piperidin-4-yloxy)-phenyl]-4,4-dimethyl-4,5-dihydro-2H-pyridazin-3-one **17b**. Compound **17b** met discovery flow criteria, demonstrated potent H₃R functional antagonism in vivo in the rat dipsogenia model and potent wake activity in the rat EEG/EMG model at doses as low as 0.1 mg/kg ip.

© 2012 Elsevier Ltd. All rights reserved.

The histamine H₃ receptor (H₃R) functions in the brain both as an autoreceptor modulating histamine release and as an inhibitory heteroreceptor regulating the release of multiple

neurotransmitters, including acetylcholine, dopamine, norepinephrine and serotonin thought to be involved in attention, sleep and cognition.¹ Activation of the H₃R results in the inhibition of

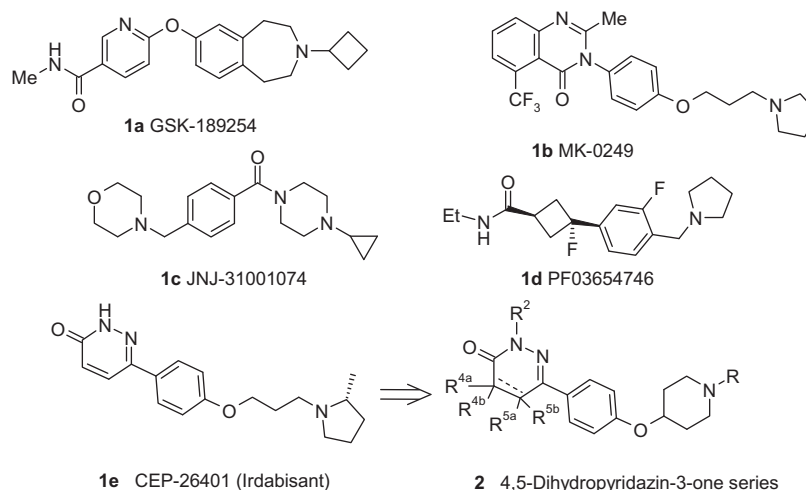
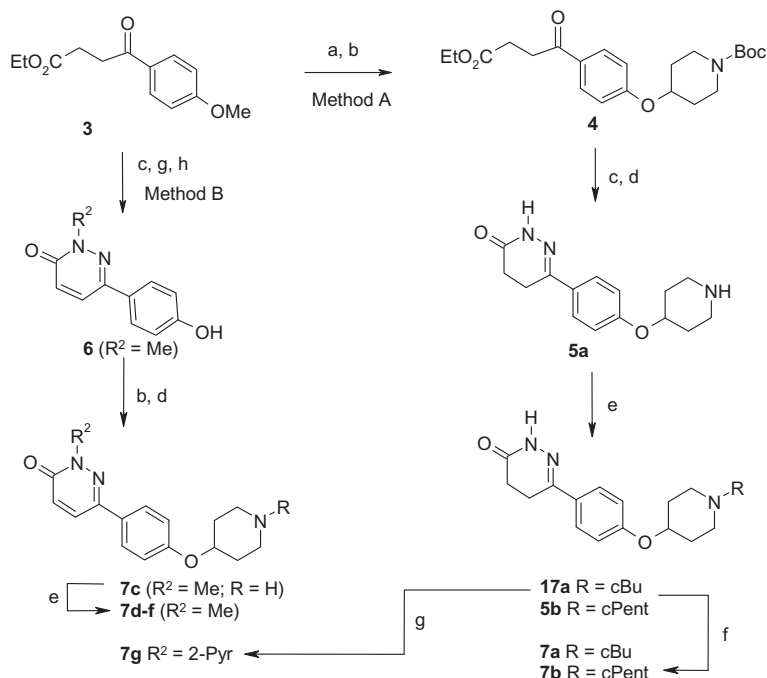


Figure 1. Structures of clinical candidates and 4,5-dihydropyridazin-3-one core.

* Corresponding author.

E-mail address: rhudkins@cephalon.com (R.L. Hudkins).



Scheme 1. Reagents and conditions: (a) (i) 48% HBr, reflux, (ii) EtOH, 94%; (b) 4-hydroxy-1-Boc-piperidine, PPh₃, THF, DEAD, rt, 92%; (c) NH₂NH₂, or MeNHNH₂, 2-propanol, reflux, R² = H 50%, R² = Me 94%; (d) TFA, DCM, 25 °C, 100%; (e) cyclobutanone or, cyclopentanone, NaCNBH₃, DMF, MeOH, AcOH, 60 °C, 34–42%; (f) Cs₂CO₃, DMSO, air, 130 °C, 33–37%; (g) MnO₂, xylenes, 155 °C, 75%; (h) BBr₃, DCM, 5 °C → rt, 98%; (g) 2-bromopyridine, K₂CO₃, CuI, DMF, 150 °C, 45%.

Table 1
Pyridazin-3-one H₃R binding data^a

Entry	R ²	R ⁵	R	hH ₃ R (K _i) (nM)	rH ₃ R (K _i) (nM)
1e				2.0	7.2
7a	H	H	cButyl	1.9	2.2
7b	H	H	cPentyl	5.1	7.0
7c	Me	H	H	695	>1000
7d	Me	H	iPr	9.2	46
7e	Me	H	cButyl	2.4	3.1
7f	Me	H	cPentyl	2.7	6.0
7g	2-Pyr	H	cButyl	9.8	15
7h	H	Me	cButyl	4.4	6.3

^a K_i Values are an average of two or more determinations. The assay-to-assay variation was typically within 2.5-fold; 2-Pyr = 2-pyridyl.

neurotransmitter release, while blockade of H₃R by selective antagonists or inverse agonists reverses histamine-mediated inhibition and enhances neurotransmitter release. Clinically H₃R antagonists are of interest for potential treatment of multiple CNS disorders associated with attention and cognitive deficits, including sleep/wake activity, attention-deficit hyperactivity disorder (ADHD), Alzheimer's disease (AD), mild cognitive impairment, and the cognitive deficits in schizophrenia.¹ Several clinical candidates (**1a–1e**) have advanced into trials (Fig. 1).^{1a,f–l} We recently disclosed a novel class of pyridazin-3-one H₃R antagonists/inverse agonists and the profile of the first clinical compound **1e** (CEP-26401, iridabisant).² A series of publications outlined the pyridazinone phenoxypropyl amine structure–activity relationships (SAR)

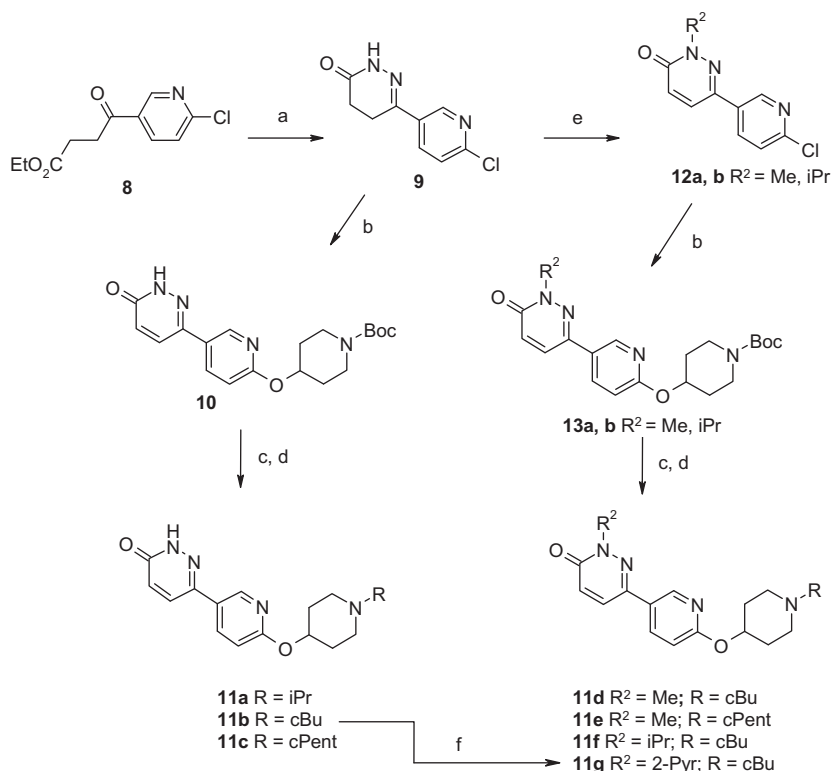
Table 2
Central ring pyridyl analogs^a

Entry	R ²	R	hH ₃ R (K _i) (nM)	rH ₃ R (K _i) (nM)
11a	H	iPr	15	101
11b	H	cButyl	6.3	19
11c	H	cPentyl	26	51
11d	Me	cButyl	1.8	8.6
11e	Me	cPentyl	5.9	12
11f	iPr	cButyl	6.5	9.4
11g	2-Pyr	cButyl	34	82

^a K_i Values are an average of two or more determinations. The assay-to-assay variation was typically within 2.5-fold; 2-Pyr = 2-pyridyl.

including the 4,5-dihydropyridazin-3-one series and amine replacements.³ An exhaustive SAR direction investigated to identify second-generation pyridazinone H₃R antagonists to iridabisant was to replace the 4-phenoxypropylamine with the conformationally restricted 4-phenoxy-piperidine fragment in both the pyridazin-3-one and non-aromatic 4,5-dihydropyridazin-3-one subseries **2**. A similar maneuver was explored by the Merck and Johnson and Johnson groups on their respective cores.⁴ In this Letter, we report the identification and potent wake promoting profile of 6-[4-(1-cyclobutyl-piperidin-4-yloxy)-phenyl]-4,4-dimethyl-4,5-dihydro-2H-pyridazin-3-one **17b**.

The 6-[4-(piperidin-4-yloxy)-phenyl]-pyridazin-3-ones **7a–f** were synthesized using a Mitsunobu reaction as outlined in Scheme 1.^{3b,5} The pyridazinone NH analogs **7a** and **7b** were synthesized via intermediate **4**, which was produced in three steps from 4-(4-methoxy-phenyl)-4-oxo-butyrac acid ethyl ester **3** (Method



Scheme 2. Reagents and conditions: (a) $\text{NH}_2\text{NH}_2 \cdot \text{H}_2\text{O}$, EtOH, 80 °C, 79%; (b) 4-hydroxy-1-Boc-piperidine, 1 M KOTBu, DMSO, 100 °C, 100%; (c) 4 N HCl, dioxane, 50 °C, 100%; (d) acetone (**11a**), cyclobutanone (**11b,d**), cyclopentanone (**11c,e**), NaCNBH_3 , DMF, MeOH, AcOH, 80 °C, 10–30%; (e) MeI or *i*PrI, Cs_2CO_3 , DMSO, air, 100 °C, 79%; (f) 2-bromopyridine, K_2CO_3 , CuI, DMF, 150 °C, 33%.

A). Intermediate **4** was condensed with hydrazine to give the 4,5-dihydropyridazinone intermediate, followed by deprotection of the Boc with TFA to produce **5a**. Reductive amination of **5a** with cyclobutanone or cyclopentanone gave 4,5-dihydropyridazinones **17a** and **5b**, respectively. Oxidation of **17a** and **5b** (DMSO/cesium carbonate) gave targets **7a** and **7b** in low yield. The route to *N*- R^2 -methyl pyridazinone targets **7d–f** was accomplished using Method B (Scheme 1). Phenol **6** was produced in three steps from **3** and then converted to **7c** via Mitsunobu reaction with 4-hydroxy-1-boc-piperidine and Boc deprotection as described previously. Reductive amination with piperidine **7c** and acetone, cyclobutanone or cyclopentanone gave targets **7d–f**. The *N*- R^2 2-pyridyl analog **7g** was synthesized from the 4,5-dihydropyridazinone **17a** and 2-bromopyridine via copper mediated coupling (Scheme 1). The central ring 3-pyridyl analogs **11a–g** in Table 2 were synthesized as outlined in Scheme 2. 4-(6-Chloro-pyridin-3-yl)-4-oxo-butyric acid ethyl ester **8** was reacted with hydrazine hydrate to produce 6-(6-chloro-pyridin-3-yl)-4,5-dihydro-2H-pyridazin-3-one **9** in high yield. *SnAr* reaction of **9** with 4-hydroxy-1-Boc-piperidine and KOTBu in DMSO gave aromatized pyridazinone **1**. Deprotection and reductive amination gave targets **11a–c**. The pyridazinone *N*- R^2 substituted analogs **11d–f** were synthesized by alkylation and aromatization of **9** to **12a** and **12b**. *SnAr* reaction, Boc deprotection and reductive amination as described previously gave **11d–f**. The *N*-2-pyridyl **11g** was produced by copper mediated coupling **11b** analogous to **7g**.

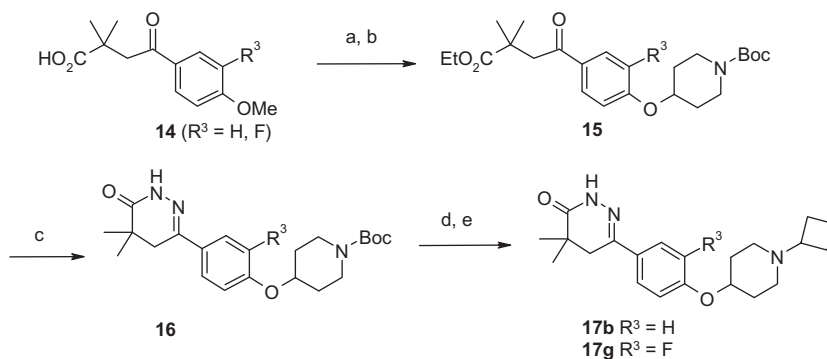
The 4,5-dihydro targets in Table 3 were synthesized using procedures outlined in Schemes 3–5. 6-[4-(1-Cyclobutyl-piperidin-4-yloxy)-phenyl]-4,4-dimethyl-4,5-dihydro-2H-pyridazin-3-one **17b** was produced from 4-(4-methoxy-phenyl)-2,2-dimethyl-4-oxo-butyric acid as outlined in Scheme 3 using analogous procedures described in Scheme 1 for **7a–f**. Likewise, 4-(3-fluoro-4-methoxy-phenyl)-2,2-dimethyl-4-oxo-butyric acid gave 3-fluoro **17g**. The

Table 3
4,5-Dihydropyridazin-3-one H_3R binding data^a

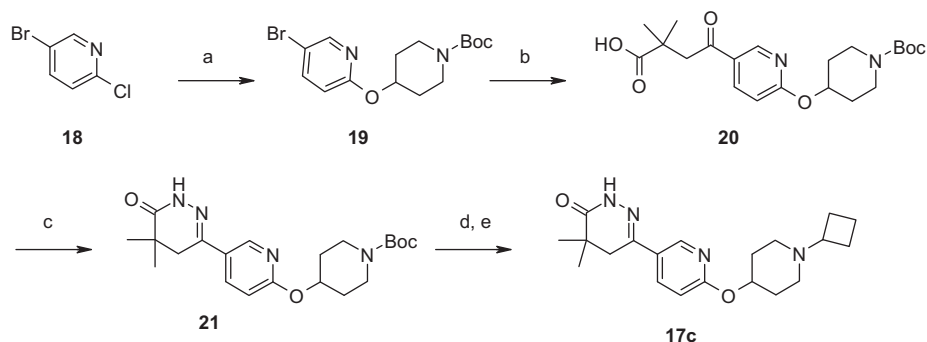
Entry	$\text{R}^{4a}/\text{R}^{4b}$	$\text{R}^{5a}/\text{R}^{5b}$	X	hH_3R (K_i) (nM)	rH_3R (K_i) (nM)
17a	H	H	CH	3.7	6.7
17b	Me/Me	H	CH	2.7	4.4
17c	Me/Me	H	N	12	28
17d	Me/Me	H	CF	7.1	7.2
R(+) 17e	H	Me	CH	5.6	9.6
S(-) 17e	H	Me	CH	7.8	13

^a K_i Values are an average of two or more determinations. The assay-to-assay variation was typically within 2.5-fold.

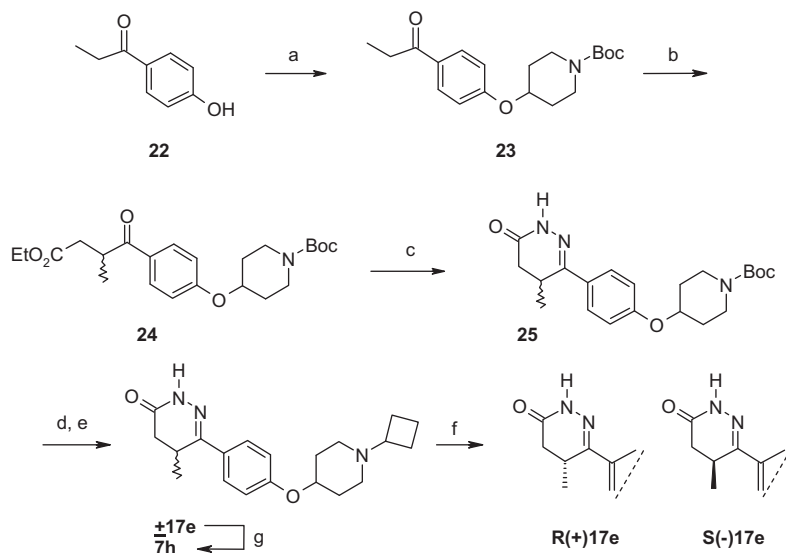
4,4-dimethyl pyridyl **17c** was produced starting with 5-bromo-2-chloro-pyridine as shown in Scheme 4. The key step was conversion of **19** to **20** via metal halogen exchange and reaction of the 3-lithiopyridyl intermediate with 3,3-dimethylsuccinic anhydride. The 5-methyl racemate **17e** was synthesized in five efficient steps starting with 1-(4-hydroxyphenyl)-propan-1-one (Scheme 5). Compound **17e** was separated using chiral SCF chromatography to give both isomers >99% ee. The structure of peak 2 (ChiraPak 1A 4.6 × 250 mm, 2.5 mL/min, 55% MeOH/0.3% DEA, peak 1 $\text{rt} = 3.2$ min, peak 2 $\text{rt} = 6.2$ min) as the HCl salt was solved by single crystal X-ray crystallography and the stereochemistry assigned as the 5-*S*-methyl isomer. The specific rotations were, peak 1 **R(+)**-**17** $[\alpha]_{\text{D}}^{24} + 30.5$ (c 0.1, MeOH) and peak 2 **S(-)**-**17** $[\alpha]_{\text{D}}^{24} - 29.2$ (c 0.1, MeOH).



Scheme 3. Reagents and conditions: (a) (i) 48% HBr, reflux, (ii) ethanol 90%; (b) 4-hydroxy-1-Boc-piperidine, PPh₃, THF, DEAD, $R^3 F = 45\%$, $R^3 H = 93\%$; (c) NH₂NH₂, 2-propanol, reflux, 89%; (d) TFA, DCM, 25 °C, 100%; (e) cyclobutanone, NaCNBH₃, DMF, MeOH, AcOH, 60 °C, 35–58%.



Scheme 4. Reagents and conditions: (a) 4-Hydroxy-1-Boc-piperidine, 1 M KOtBu, toluene, 80 °C, 68%; (b) 3,3-dimethyl-dihydro-furan-2,5-dione, 1.4 M sec-BuLi, ether, –78 °C, 35%; (c) NH₂NH₂·H₂O, 2-propanol, 120 °C, 97%; (d) TFA, DCM, 25 °C, 100%; (e) cyclobutanone, NaCNBH₃, DMF, MeOH, AcOH, 60 °C, 65%.



Scheme 5. Reagents and conditions: (a) 4-Hydroxy-1-Boc-piperidine, PPh₃, THF, DEAD, 60%; (b) LDA, ethyl bromoacetate, THF, 0 °C; (c) NH₂NH₂·H₂O, 2-propanol, 110 °C, 65% two steps; (d) TFA, DCM, 25 °C, 100%; (e) cyclobutanone, NaCNBH₃, DMF, MeOH, AcOH, 60 °C, 60% two steps; (f) SCF chiral separation; (g) Cs₂CO₃, DMSO, air, 100 °C, 94%.

The phenoxy-piperidine–pyridazinone analogs were tested using *in vitro* binding assays by displacement of [³H]NAMH in membranes isolated from CHO cells transfected with cloned human H₃ or rat H₃ receptors as shown in Tables 1–3.^{2,3} Replacing the *R*-2-methyl-pyrrolidinyl propoxy fragment of iridabisant **1e** with *N*-cyclobutylpiperidinyl (**7a** hH₃R $K_i = 1.9$ nM, rH₃R $K_i = 2.2$ nM) and *N*-cyclopentylpiperidinyl (**7b** hH₃R $K_i = 5.1$ nM,

rH₃R $K_i = 7.0$ nM) showed comparable affinity (Table 1). Likewise, the *N*-methyl pyridazinones **7e** and **7f** were equally well tolerated,^{3b} although the 2-pyridyl **7g** had slightly weaker H₃R binding affinity. The SAR at the piperidine nitrogen with compounds **7c–f** showed that the cyclobutyl was optimum. The *N*-isopropyl **7d** produced a large drop in affinity compared to *N*-cyclobutyl **7e**, while the piperidine NH compound **7c** was essentially inactive. Com-

Table 4
Pharmacokinetic properties in rat^a

		7a	17b	S-17e
iv	$t_{1/2}$ (h)	2.3 ± 0.4	1.9 ± 0.9	4.4 ± 1.2
	V_d (L/kg)	2.5 ± 0.6	3.1 ± 0.4	7.6 ± 0.3
po	CL (mL/min/kg)	13 ± 3	18 ± 2	23 ± 6
	AUC	1535 ± 117	1235 ± 162	1226 ± 78
C_{max} (ng/mL)		441 ± 22	270 ± 47	253 ± 21
	F (%)	35 ± 1	33 ± 4	56 ± 5
	B/P ^b	1.9 ± 0.1	4.0 ± 0.6	5.3 ± 0.3

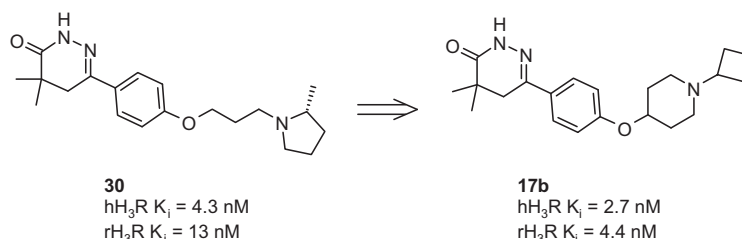
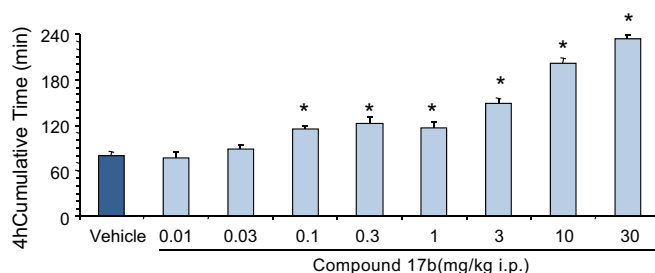
^a Administration at 1 mg/mg iv and 5 mg/kg po; iv formulation (3% DMSO, 30% solutol, 67% phosphate buffered saline) oral formulation (50% Tween 80, 40% propylene carbonate and 10% propylene glycol).

^b B/P = brain to plasma ratio measured 6 h post 10 mg/kg ip dose.

Compound **7a** from this set was selected for additional profiling to identify potential issues and areas of improvement as a backup to iridabisant. Compound **7a** was a potent, full inverse agonist in the [³⁵S]GTP γ S hH₃R binding assay (EC_{50} = 1.1 nM)² and displayed acceptable drug-like properties with low lipophilicity ($clogP$ = 1.5), high permeability (Caco-2 P_{app} = 16.5×10^{-6} cm/s) and water solubility (pH 2 and pH 7.4 > 1 mg/mL). Compound **7a** showed acceptable in vitro metabolic stability across species in liver microsomes ($t_{1/2}$ > 40 min in mouse, rat, dog, monkey and human) and IC_{50} values >30 μ M for inhibition of cytochrome P450 enzymes (CYP1A2, 2C9, 2C19, 2D6 and 3A4), indicating low potential for drug–drug interactions. Compound **7a** displayed excellent selectivity over hH₁, hH₂, and hH₄ receptor subtypes (<10% inhibition at 10 μ M) and when screened against a panel of 63 GPCRs, ion channels and enzymes it showed activity only for the dopamine transporter (DAT, 63% inhibition at 10 μ M; MDS Pharma Services, LeadProfile screen). The hERG IC_{50} was 8 μ M in a patch clamp assay. The pharmacokinetic (PK) profile in rat showed **7a** had a iv half-life of 2.3 h, moderate clearance and acceptable oral bioavailability and brain exposure (brain concentration 6 h following a 5 mg/kg po dose = 1.4 μ M) (Table 4). The hERG selectivity and the DAT activity required further improvement for a compound to be considered as a potential backup/second generation wake promoting agent to iridabisant.^{2a}

The SAR of the central pyridyl analogs, designed to lower the $clogP$ and potentially improve hERG activity, is shown in Table 2. In general, parallel changes in the pyridyl series showed weaker affinity compared to the phenyl series (compare **11b** to **7a**, and **11c** to **7b**). Pyridyl **11b** ($clogP$ = 0.9) retained high affinity for hH₃R, but unfortunately did not show an improvement in hERG selectivity (IC_{50} = 9 μ M) or rat oral bioavailability (% F = 21). Of note, an opposite SAR trend was observed compared to the phenyl series when changing the NH-pyridazinone to an *N*-methyl (compare **11d** to **11b**, and **11e** to **11c**).

We recently reported a series of non-aromatic 4,5-dihydropyridazin-3-one phenoxypropylamines and the wake promoting activity of compound **30** (Fig. 2).^{3f} A key issue in the phenoxypropyl series was blocking in vivo metabolism of the 4,5-dihydropyridazinone ring. A similar SAR was explored on the phenoxypropylamine core for comparison. 4,5-Dihydro-2H-pyridazin-3-one **17a** had

**Figure 2.** Design of **17b** based on profile of **30**.**Figure 3.** Compound **17b**-induced wake promotion. Cumulative time awake for 4 h (4 h AUC) following administration of vehicle or compound **17b** in chronically implanted rats. Mean \pm SEM, n = 8–14/group. * p < 0.05, Dunnett's post-hoc test versus vehicle.

high H₃R affinity, but as we observed in the phenoxypropyl series, in vivo metabolite identification (ID) studies revealed **17a** was metabolized approximately 35% to **7a** in the rat, and about 20–25% in the dog. Based on the formation of an undesired active H₃R metabolite, and findings with the phenoxypropyl series, we next installed the 5-methyl to potentially block in vivo metabolite formation.^{3f} Isomers **R-17e** and **S-17e** (Table 3) showed comparable H₃R binding affinity (Table 3), selectivity, functional activity (**R-17e** $K_{b,app}$ = 0.6, EC_{50} = 1.3 nM; **S-17e** $K_{b,app}$ = 0.7 nM, EC_{50} = 1.6 nM) and pharmacokinetics in rat (**S-17e**, Table 4). The in vivo rat metabolite ID study revealed **R-17e** was metabolized about 25% to **7h** following oral administration, while the *S*-isomer was stable. Further profiling showed incorporation of the *S*-methyl (**S-17e**) improved hERG activity (IC_{50} = 27 μ M) and DAT selectivity (13% inhibition at 10 μ M) compared to **7a**. However, this compound was later abandoned due to concerns with the fate of the *S*-isomer in higher species.

Subsequently, the 4,4-dimethyl phenoxypropylamine analog of **30**^{3f} was synthesized and profiled (Fig. 2). Compound **17b** had high affinity for both human and rat H₃R, while the 3-pyridyl **17c** and 3-fluoro **17d** had slightly weaker binding affinity. Functionally, **17b** was a full inverse agonist (EC_{50} = 0.8 nM) and showed acceptable in vitro metabolic stability ($t_{1/2}$ > 40 min across species), and cytochrome P450 selectivity (IC_{50} > 30 μ M). The hERG IC_{50} value was 21 μ M and selectivity profiling showed **17b** had >1000-fold selectivity against hH₁, hH₂, and hH₄ receptor subtypes and against a panel of 172 GPCRs, ion channels and enzymes (<50% inhibition at 10 μ M; DAT = 8%; MDS Pharma Services, LeadProfiler and Spectrum screen). The permeability was classified as high (Caco2 P_{app} = $27 \pm 0.4 \times 10^{-6}$ cm/s) and plasma protein binding for rat, dog, and human was low to moderate (50–60%). In rat PK studies it showed an iv $t_{1/2}$ < 2 h, with acceptable oral bioavailability and brain exposure (brain concentration 6 h following a 5 mg/kg po dose = 2.1 μ M) (Table 4).

Compound **17b** met all discovery criteria and advanced into in vivo evaluation in the rat dipsogenia and the rat EEG/EMG sleep–wake models. The rat dipsogenia model was used as an in vivo surrogate measure of H₃R functional inhibition in the brain following peripheral administration. Histamine and the

H₃-selective agonist, *R*- α -methylhistamine (RAMH), induce water drinking in the rat when administered either peripherally or centrally, an effect that is blocked by H₃R antagonists.^{1k,2,6} Compound **17b** potently and dose-dependently inhibited RAMH-induced dipsogenia with an ED₅₀ value of 0.14 mg/kg ip. H₃R antagonists including irdabisant and its analogs demonstrated wake promoting activity in the rat.^{2b,3a,3f,7} Wake-promoting activity of **17b** in the rat was measured from 0.01 to 30 mg/kg ip as previously described using rats surgically implanted for chronic recording of EEG (electroencephalographic) and EMG (electromyographic) signals enabling wake, slow-wave sleep, and rapid eye-movement sleep to be scored by standard criteria.^{2b,8,9} The cumulative wake time at 4 h after dosing (5 h after lights on) was evaluated during the normal quiet period of the rat. Compound **17b** significantly and dose-dependently increased wake at doses from 0.1 up to 30 mg/kg ip by 4 h AUC values ($P < 0.001$ ANOVA) (Fig. 3). Doses of 0.1–1 mg/kg increased wake 45–50% above the vehicle value, from 80 \pm 5 min (vehicle group) to 115 \pm 4 (0.1 mg/kg), 122 \pm 9 min (0.3 mg/kg), and 116 \pm 7 min (1 mg/kg). At 10 mg/kg, percent time awake was maintained over 90% for the first 2 h after dosing. Wake in the 10 and 30 mg/kg groups was increased to 201 \pm 7 and 234 \pm 4 min at 4 h (152% and 193%, respectively, compared to vehicle, equivalent to 84% and 98% time awake for 4 h). At 30 mg/kg, maximal cumulative wake surplus (excess wake time compared to the vehicle group) was 196 min at 7 h post dosing, which was maintained up to 22 h. Sleep rebound was not observed in any of the treatment groups. Compound **17b** thus demonstrated very potent wake promotion in rat at doses as low as 0.1 mg/kg ip and robust wake at higher doses.

In summary, optimization of the phenoxypiperidine core led to the identification of target molecules meeting H₃R target potency, selectivity and rat pharmacokinetic criteria. The search for compounds with improved hERG and DAT selectivity and lacking in vivo active metabolites identified 6-[4-(1-cyclobutyl-piperidin-4-yloxy)-phenyl]-4,4-dimethyl-4,5-dihydro-2*H*-pyridazin-3-one **17b**. Compound **17b** met all discovery criteria, including demonstration of potent functional H₃R antagonism in vivo in the rat dipsogenia model and potent wake activity in the rat EEG/EMG model at doses as low as 0.1 mg/kg ip.

Acknowledgments

The authors thank Emily Kordwitz, Mark Olsen, Gilbert Moachon, Nicole Lepallec, Isabelle Kanmacher, Véronique Agathon, Mehran Yazdani and Val Marcy for their assistance and support.

References and notes

- Reviews: (a) Berlin, M.; Boyce, C. W.; de Lera Ruiz, M. J. *Med. Chem.* **2011**, *54*, 26; (b) Leurs, R.; Bakker, R. A.; Timmerman, H.; de Esch, I. J. *Nat. Rev. Drug Discov.* **2005**, *4*, 107; (c) Wijnmans, M.; Leurs, R.; de Esch, I. *Expert Opin. Investig. Drugs.* **2007**, *16*, 967; (d) Esbenshade, T. A.; Fox, G. B.; Cowart, M. D. *Mol. Interv.* **2006**, *6*, 77; (e) Esbenshade, T. A.; Browman, K. E.; Bitner, R. S.; Strakhova, M.; Cowart, M. D.; Brioni, J. D. *Br. J. Pharmacol.* **2008**, *154*, 1166; (f) Hudkins, R. L.; Raddatz, R. *Ann. Rep. Med. Chem.* **2007**, *42*, 49; (g) Raddatz, R.; Tao, M.; Hudkins, R. L. *Curr. Top. Med. Chem.* **2010**, *10*, 153; (h) Brioni, J. D.; Esbenshade, T. A.; Garrison, T. R.; Bitner, S. R.; Cowart, M. D. *J. Pharmacol. Exp. Ther.* **2011**, *336*, 38; (i) Medhurst, A. D.; Atkins, A. R.; Beresford, I. J.; Brackenborough, K.; Briggs, M. A.; Calver, A. R.; Cilia, J.; Cluderay, J. E.; Crook, B.; Davis, J. B.; Davis, R. K.; Davis, R. P.; Dawson, L. A.; Foley, A. G.; Gartlon, J.; Gonzalez, M. I.; Heslop, T.; Hirst, W. D.; Jennings, C.; Jones, D. N.; Lacroix, L. P.; Martyn, A.; Ociepka, S.; Ray, A.; Regan, C. M.; Roberts, J. C.; Schogger, J.; Southam, E.; Stean, T. O.; Trail, B. K.; Upton, N.; Wadsworth, G.; Wald, J. A.; White, T.; Witherington, J.; Woolley, M. L.; Worby, A.; Wilson, D. M. *J. Pharmacol. Exp. Ther.* **2007**, *1032*, 321; (j) Nagase, T.; Mizutani, T.; Ishikawa, S.; Sekino, E.; Sasaki, T.; Fujimura, T.; Ito, S.; Mitobe, Y.; Miyamoto, Y.; Yoshimoto, R.; Tanaka, T.; Ishihara, A.; Takenaga, N.; Tokita, S.; Fukami, T.; Sato, N. *J. Med. Chem.* **2008**, *51*, 4780; (k) Thompson Reuters Integrity, Bavisant, entry 470497, 2011; (l) Thompson Reuters Integrity, MK-0249, entry 433171, 2011.
- (a) Hudkins, R. L.; Raddatz, R.; Tao, M.; Mathiasen, J. R.; Aimone, L. D.; Becknell, N. C.; Prouty, C. P.; Knutsen, L.; Yazdani, M.; Moachon, G.; Ator, M. A.; Mallamo, J. P.; Marino, M. J.; Bacon, E. R.; Williams, M. J. *Med. Chem.* **2011**, *54*, 4781; (b) Raddatz, R.; Hudkins, R. L.; Mathiasen, J. R.; Gruner, J. A.; Flood, D. G.; Aimone, L. D.; Le, S.; Schaffhauser, H.; Gasior, M.; Bozyczko-Coyne, D.; Marino, M. J.; Ator, M. A.; Bacon, E. R.; Mallamo, J. P.; Williams, M. J. *Pharmacol. Exp. Ther.* **2012**, *340*, 124.
- (a) Hudkins, R. L.; Aimone, L. D.; Bailey, T. R.; Bendesky, R. J.; Dandu, R.; Dunn, D.; Gruner, J. A.; Josef, K. A.; Lin, Y.-G.; Lyons, J.; Marcy, V. R.; Mathiasen, J. R.; Sundar, B. G.; Tao, M.; Zulli, A. L.; Rita Raddatz, R.; Bacon, E. R. *Bioorg. Med. Chem. Lett.* **2011**, *21*, 5493; (b) Sundar, B. G.; Bailey, T.; Bacon, E.; Aimone, L.; Huang, Z.; Lyons, J.; Raddatz, R.; Hudkins, R. L. *Bioorg. Med. Chem. Lett.* **2011**, *21*, 5543; (c) Tao, M.; Raddatz, R.; Aimone, L. D.; Hudkins, R. L. *Bioorg. Med. Chem. Lett.* **2011**, *21*, 6126; (d) Dandu, R.; Gruner, J. A.; Mathiasen, J. R.; Aimone, L. D.; Hosteller, G.; Benfield, C.; Bendesky, R. J.; Marcy, V. R.; Raddatz, R.; Hudkins, R. L. *Bioorg. Med. Chem. Lett.* **2011**, *21*, 6362; (e) Becknell, N. C.; Lyons, J.; Aimone, L. D.; Gruner, J. A.; Mathiasen, J. R.; Rita Raddatz, R.; Hudkins, R. L. *Bioorg. Med. Chem. Lett.* **2011**, *21*, 7076; (f) Hudkins, R. L.; Aimone, L. D.; Dandu, R.; Dunn, D.; Gruner, J. A.; Huang, Z.; Josef, K. A.; Lyons, J.; Mathiasen, J. R.; Tao, M.; Zulli, A. L.; Raddatz, R. *Bioorg. Med. Chem. Lett.* **2012**, *22*, 194.
- (a) Dvorak, C. A.; Apodaca, R.; Barbier, A. J.; Berridge, C. W.; Wilson, S. J.; Boggs, J. D.; Xiao, W.; Lovenberg, T. W.; Carruthers, N. I. *J. Med. Chem.* **2005**, *48*, 2229; (b) Nagase, T.; Mizutani, T.; Sekino, E.; Ishikawa, S.; Ito, S.; Mitobe, Y.; Miyamoto, Y.; Yoshimoto, R.; Tanaka, T.; Ishihara, A.; Takenaga, N.; Tokita, S.; Sato, N. *J. Med. Chem.* **2008**, *51*, 6889.
- Bacon, E. R.; Bailey, T. R.; Becknell, N. C.; Chatterjee, S.; Dunn, D.; Hostetler, G. A.; Hudkins, R. L.; Josef, K. A.; Knutsen, L.; Tao, M.; Zulli, A. L.; US2010273779, 2010.
- Clapham, J.; Kilpatrick, G. J. *Eur. J. Pharmacol.* **1993**, *232*, 99.
- Lin, J. S.; Sergeeva, O. A.; Haas, H. L. *J. Pharmacol. Exp. Ther.* **2011**, *336*, 17.
- Le, S.; Gruner, J. A.; Mathiasen, J. R.; Marino, M. J.; Schaffhauser, H. *J. Pharmacol. Exp. Ther.* **2008**, *325*, 902.
- (a) Edgar, D. M.; Seidel, W. F. *J. Pharmacol. Exp. Ther.* **1997**, *283*, 757; (b) Opp, M. R.; Krueger, J. M. *Brain Res.* **1994**, *639*, 57.